RESEARCH PAPER

Simple Preparation of Magnetic, Antibacterial and Photo-catalyst NiFe$_2$O$_4$@TiO$_2$/Pt Nanocomposites

Gholamreza Nabiyouni [1,2,*], Davood Ghanbari [3]

[1] *Department of Physics, Faculty of Science, Arak University, Arak, Iran*

[2] *Institute of Nanoscience and Nanotechnology, Arak University, Arak, Iran*

[3] *Department of Science, Arak University of Technology, Arak, Iran*

ARTICLE INFO

ABSTRACT

Firstly nickel ferrite nanoparticles were synthesized via a simple precipitation method. Then mono-disperse platinum nanoparticles and NiFe$_2$O$_4$@TiO$_2$/Pt nanocomposites were synthesized by a facile sol-gel procedure. The structure, phase and crystallite size of the magnetic and photo-catalyst products were characterized by X-ray diffraction pattern (XRD). The morphology and size of the nanostructures were surveyed by scanning electron microscopy (SEM). The purity of the samples was confirmed by Fourier transform infrared (FT-IR) spectroscopy. Vibrating sample magnetometer (VSM) illustrated that nickel ferrite nanoparticles have super paramagnetic behaviour. The photo catalytic behaviour of NiFe$_2$O$_4$@TiO$_2$/Pt nanocomposites was approved using the fast degradation of two various azo dyes under visible and ultra violet light irradiation. The results show that nanocomposites have feasible magnetic feature for easy separation and effective photo catalytic properties for purification of organic dye contaminants. The antibacterial behaviour of NiFe$_2$O$_4$@TiO$_2$/Pt nanocomposites was evaluated using degradation of E coli bacteria.

INTRODUCTION

Nickel ferrite (NiFe$_2$O$_4$) is an inverse spinel that the cubic unit cell is formed by 56 atoms, 32 oxygen anions dispersed in a cubic close packed structure. It is a kind of soft magnetic materials with many merits, such as abundant source, low price, high electrical resistance, chemical and mechanical stability and widely used in high dense magnetic recording media, magnetic fluids and high frequency equipment [1-3]. Platinum nanoparticles can absorb visible light due to their localized surface plasmon resonance (LSPR). When the frequency of the light satisfies the resonance conditions of the platinum nanoparticles, the LSPR occurs with the associated light absorption. Platinum nanoparticles can also work as an electron trap and active reaction sites. It was explored the applicability of plasmonic processes in the field of photocatalytic chemistry for toxic organic decomposition. Simultaneous of LSPs other effects such as optical near-field enhancement, heat generation and excitation of hot-electrons occur. The composites of semiconductor nanoparticles and optically active metallic nanostructures show suitable application in comparison to conventional photocatalysts. The main feature of these photocatalysts is that the interaction between semiconductor and metallic building blocks results in very efficient conversion of incident photons into electron-hole pairs in the semiconductor [4-12].

In this work NiFe$_2$O$_4$ nanoparticles were

* Corresponding Author Email: g-nabiyouni@araku.ac.ir

synthesized by simple precipitation method. Then NiFe$_2$O$_4$@TiO$_2$/Pt nanocomposites were synthesized by a facile sol-gel procedure. The photo catalytic behaviour of NiFe$_2$O$_4$/Pt nanocomposites was evaluated using the degradation of two azo dyes under ultraviolet light irradiation. The results show that nanocomposites have applicable super paramagnetic, antibacterial and photo catalytic performance.

MATERIALS AND METHODS

Ni(NO$_3$)$_2$, Fe(NO$_3$)$_3$ 9H$_2$O , K$_2$PtCl$_4$, NaBH$_4$, ammonia and de-ionized water were purchased from Merck Company was prepared. Scanning electron microscopy images were obtained using a JEOL instrument model. All the chemicals were used as received without further purifications. Before to taking images, the samples were coated by a very thin layer of Au (using a BAL-TEC SCD 005 sputter coater) to make the sample surface conducting and prevent charge accumulation, and obtaining a better contrast. A multiwave ultrasonic generator (Bandeline MS 73), equipped with a converter/transducer and titanium oscillator, operating at 20 kHz with a maximum power output of 200 W was used for the ultrasonic irradiation. X-ray diffraction patterns were achieved by a Philips, X-ray diffractometer using Ni-filtered CuKα radiation. Room temperature magnetic properties were investigated using a vibrating sample magnetometer (VSM) device, (Meghnatis Kavir Kashan Co., Iran) in an applied magnetic field sweeping between ±10000 Oe.

Synthesis of NiFe$_2$O$_4$ nanoparticles

0.001 mol of NiSO$_4$ and 0.002 mol of Fe(NO$_3$)$_3$ 9H$_2$O were dissolved in 200 ml of distilled water. Then 10 ml of ammonia (10M) was added to the solution (pH:10) and black precipitate was prepared. After washing the magnetic precipitate was dried at 50 C for 24 h.

Synthesis of NiFe$_2$O$_4$@TiO$_2$/Pt nanocomposites

Firstly 0.1 g of synthesized nickel ferrite was dispersed in 10 ml of methanol. It was mixed on magnetic stirring for 15 min. Then 0.25g of titanium tetra isopropoxide (TTIP) (Yield of TiO$_2$: 0.1g) was added to the solution and was mixed for 10 min. After that 1ml of distilled water was added and the solution was stirred for 10 min. HNO$_3$ was slowly added to reaching pH of solution to 2. After 90 minutes stirring the gel was obtained. Then it was dried in oven for 45min and was calcinated at 500°C for 2h. Finally for platinum layer Pt ions were reduced on the surface by fresh NaBH$_4$ (0.05g was dissolved in 10ml of water) as precipitating and reducing agent (Fig. 1).
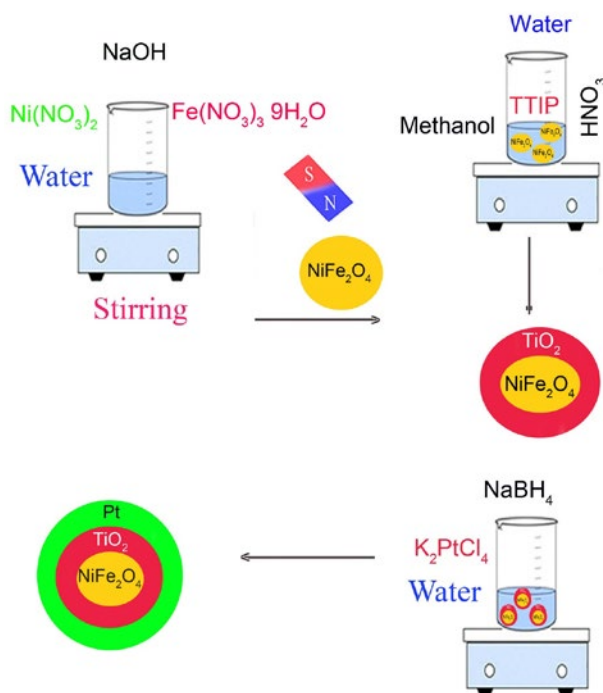

Fig. 1. Schematic of nanocomposite preparation

RESULTS AND DISCUSSION

SEM images of the as-synthesized NiFe$_2$O$_4$ nanoparticles prepared by precipitation method are illustrated in Fig. 2. Nucleation stage overcomes to growth stage the and nanoparticles with average particle size less than 40 nm were synthesized.

SEM images of the prepared NiFe$_2$O$_4$@TiO$_2$ nanoparticles by sol-gel method at 500 °C for 2h are shown in Fig. 3. Results confirm average diameter size less than 90 nm were prepared.

The particle size and morphology can be manipulated by adjusting the super-saturation during the nucleation and crystal growth in precipitation, which in turn, it can strongly be affected by solution chemistry conditions such as reaction temperature depends on precursor, time and temperature and pH of process environment.

Fig. 4 show SEM images of NiFe$_2$O$_4$@TiO$_2$/Pt nanocomposites by precipitation method with 10 ml of NaBH$_4$ as reducing agent at 180°C for 2h. Images approve formation of nanostructures with average particle size around 90 nm. The balance between nucleation rate and growth rate which determines final particle size and morphology.

Fig. 5 illustrates XRD pattern of NiFe$_2$O$_4$ product. It can be observed that cubic phase (JCPDS No. 87-0722) with Fd-3m space group which is consistent with iron was prepared. Fig. 6 shows XRD pattern of titanium dioxide product. (Pure anatase tetragonal phase with JCPDS: 04-0477 space group141/amd was prepared). Fig. 7 shows XRD pattern of platinum product. A number of strong Bragg reflection peaks can be seen which correspond to the reflections of FCC platinum. The platinum (standards JCPDS No.87-0644) and space group of Fm-3m (space group number: 225) in the pattern are reported. The calculated crystalline sizes from Scherrer equation, were about 35 and 15 nm for titanium dioxide and Pt nanoparticles, respectively.

Fig. 8 depicts the FT-IR spectrum of the NiFe$_2$O$_4$@TiO$_2$/Pt product. The absorption bands at 350-650 cm^{-1} are related to the stretching mode of Fe-O and Ni-O bonds (metal-oxygen bonds). The spectrum exhibits broad absorption a peak at 3400 cm^{-1}, corresponding to the stretching mode of adsorbed hydroxyl group. There are no other significant peaks related to precursors and other impurities.
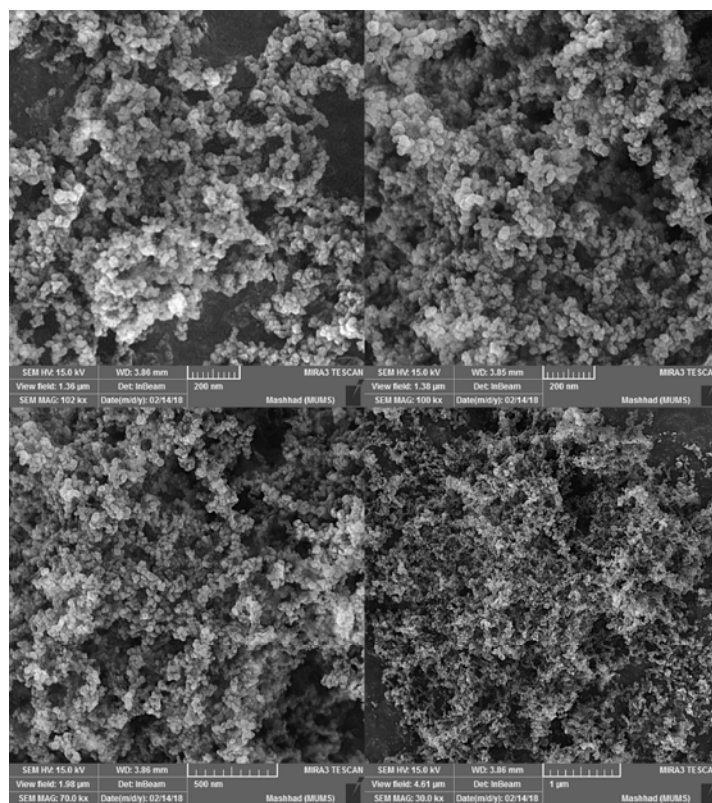

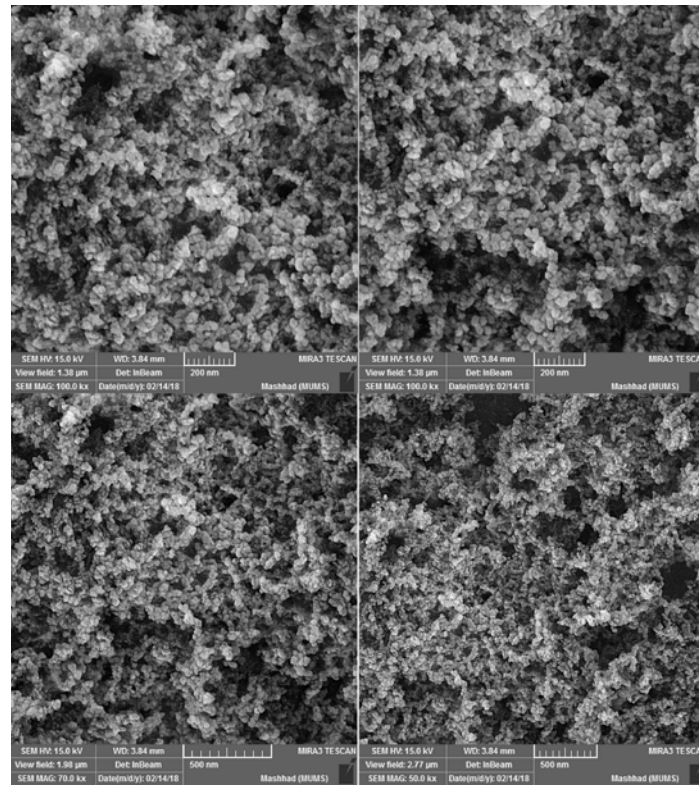Fig. 2. SEM images of NiFe$_2$O$_4$ nanoparticles synthesized by precipitation method

Fig. 3. SEM images of NiFe$_2$O$_4$@TiO$_2$ nanoparticles prepared at 500 °C

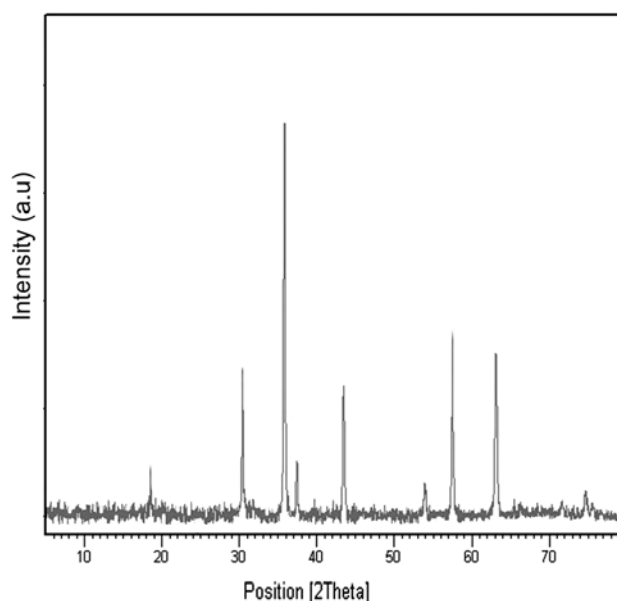Fig. 4. SEM images of NiFe$_2$O$_4$@TiO$_2$/Pt nanocomposite
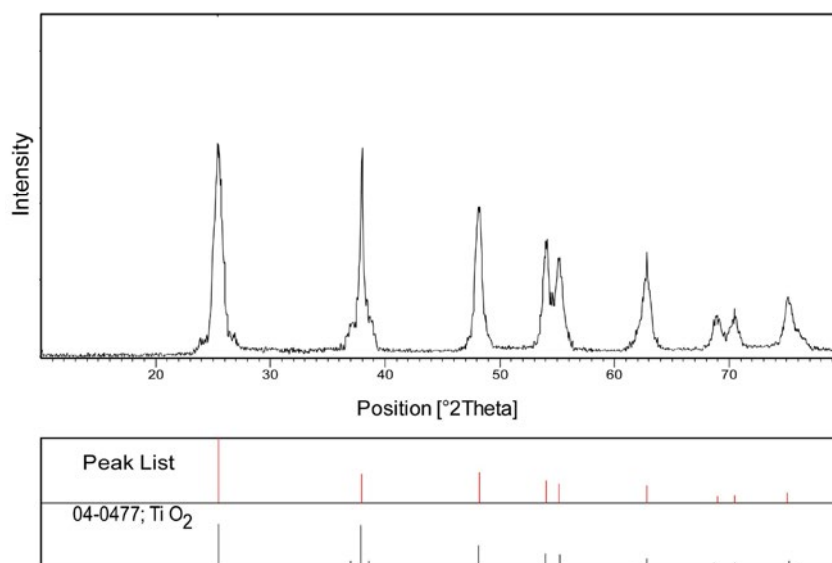
Fig. 5. XRD pattern of NiFe$_2$O$_4$ nanoparticles

Fig. 6. XRD pattern of TiO$_2$ nanoparticles

Magnetic properties of samples were studied using vibrating sample magnetometer system at room temperature. Hysteresis loop of magnetic NiFe$_2$O$_4$ nanoparticles prepared by precipitation method is shown in Fig. 9. As-synthesized nanoparticles show super paramagnetic behaviour and have a saturation magnetization of 40 emu/g and a coercivity tending to zero Oe. It shows a sufficient magnetization of these nanoparticles for being recycled by a magnet, making them

appropriate for core of recyclable photo-catalyst.

Hysteresis loop of magnetic NiFe$_2$O$_4$@TiO$_2$/Pt nanoparticles is depicted in Fig. 10. The product also illustrates super paramagnetic behaviour and has a saturation magnetization of 29 emu/g and a coercivity about zero Oe.

This magnetization indicates that NiFe$_2$O$_4$/Pt nanocomposites inherit the magnetic property from the NiFe$_2$O$_4$; however, the magnetization is lower due to presence of platinum. This reduction
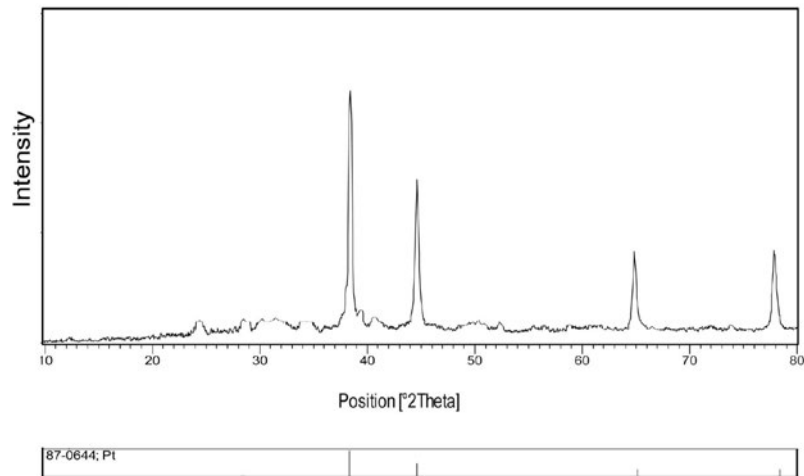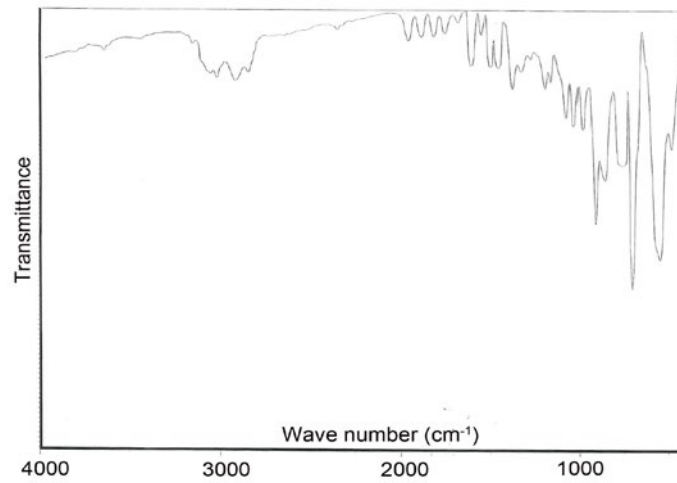
Fig. 7. XRD pattern of Pt nanoparticles

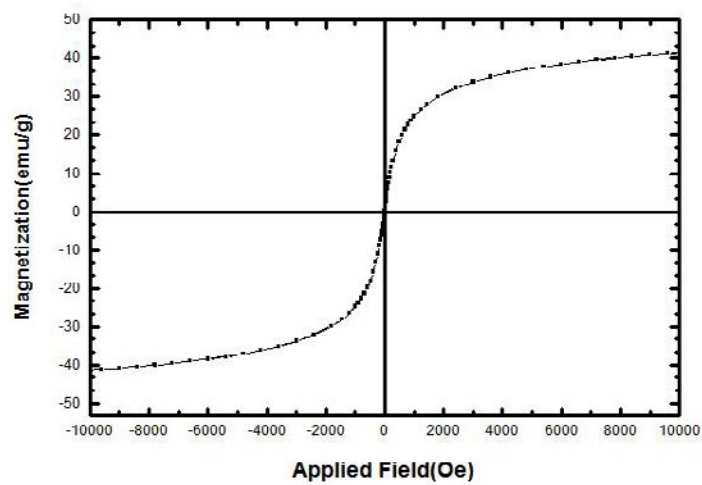Fig. 8. FT-IR spectrum of NiFe$_2$O$_4$@TiO$_2$/Pt nanocomposite

Fig. 9. Room temperature hysteresis loop of NiFe$_2$O$_4$ nanoparticles

in saturation magnetization is due to the interfacial effect of the typical nanocomposite. The magnetic property of the prepared nanocomposites is an essential characteristic of a re-generable and reusable magnetic heterogeneous catalyst.

The photo-catalytic activity of the $NiFe_2O_4@$ TiO_2/Pt nanocomposite was evaluated by monitoring the degradation of Methyl Orange and Acid-Brown in an aqueous solution, under irradiation with UV light. The photo-degradation mechanism of TiO_2-platinum under UV-visible absorption is illustrated in Fig. 11. Maximum wave length of Methyl Orange and Acid-Brown were degraded about 45% and 65% in 90 min in

the presence of iron-platinum. Methyl Orange depicted the fastest degradation at 90 min under ultraviolet light and at presence of magnetic photo-catalyst. Organic dyes decompose to carbon dioxide, water and other less toxic or nontoxic remaining and residuals [13-20]. Fig. 12 shows degradation of the three two dyes after 90 min exposure to the $NiFe_2O_4@TiO_2/Pt$ nanocomposite. The as-prepared nanocomposite has the potential to be applied to improve environmental problems associated with organic and toxic water pollutants. Antibacterial effect of $NiFe_2O_4@TiO_2/Pt$ nanocomposite on the degradation of E Coli bacteria is shown in Fig 13.
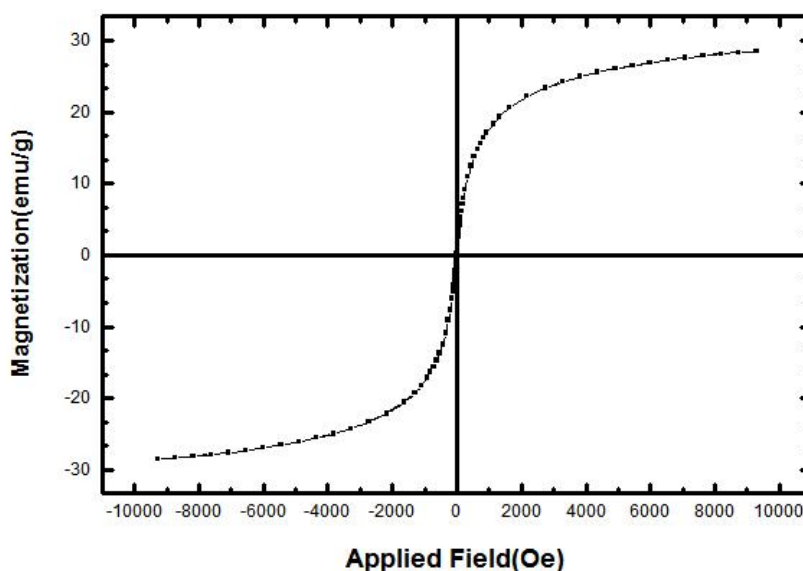

Fig. 10. Room temperature hysteresis loop of $NiFe_2O_4@TiO_2/Pt$ nanocomposite
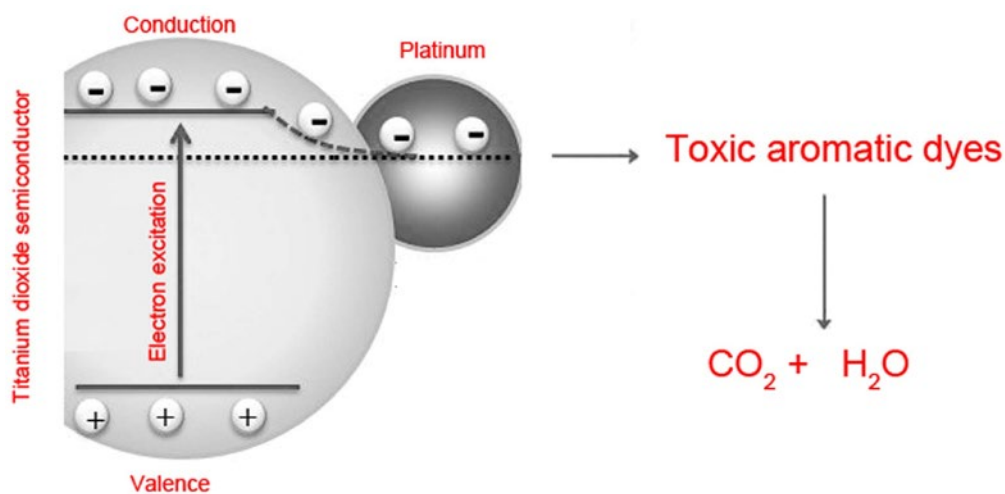

Fig. 11. Photo-catalyst mechanism of titanium dioxide- platinum in degradation of toxic dye
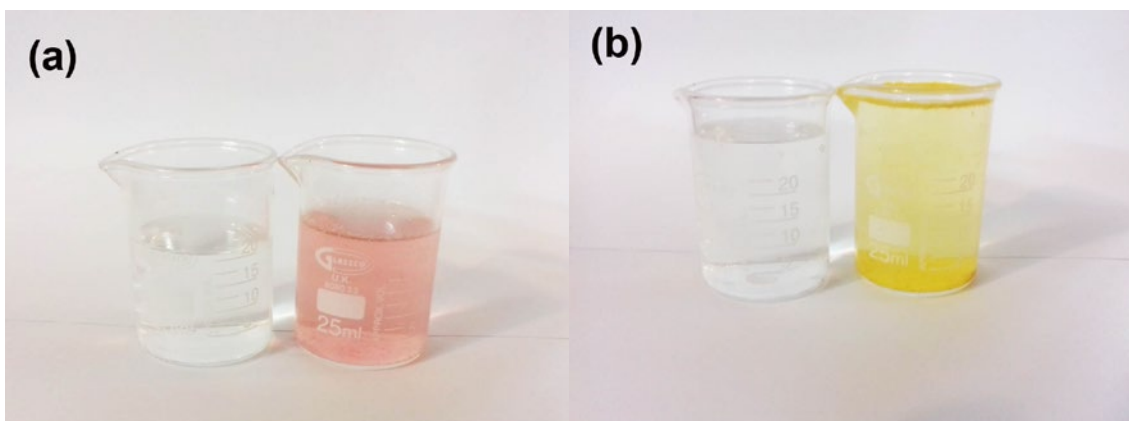
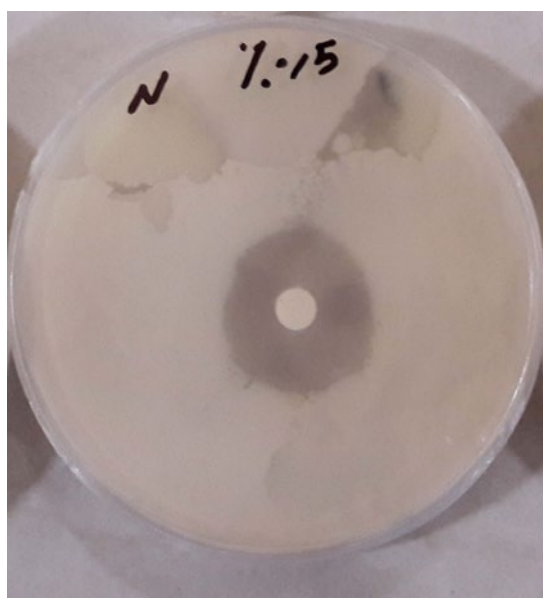Fig. 12. Photo degradation of (a) Methyl Orange (b) Acid Brown

Fig. 13. Antibacterial effect of NiFe$_2$O$_4$@TiO$_2$/Pt nanoparticles on E-Coli

As time increase; more bacteria are degraded on the nanoparticles catalyst, until obvious circle was observed around antibacterial NiFe$_2$O$_4$@TiO$_2$/Pt disk.

CONCLUSIONS

Firstly nickel ferrite nanoparticles were synthesized via a large-scale precipitation method, then platinum nanoparticles and NiFe$_2$O$_4$@TiO$_2$/Pt nanocomposites were prepared by precipitation method. Effect of temperature, reaction time and various concentration of NaBH$_4$ were investigated on the morphology and particle size of the products. Vibrating sample magnetometer confirmed that nanocomposites show superparamagnetic behaviours. The photocatalytic behaviour of NiFe$_2$O$_4$@TiO$_2$/Pt nanocomposite was evaluated using the degradation of two azo dyes under UV-visible light irradiation. The results show that precipitation and sol-gel methods are suitable method for preparation of NiFe$_2$O$_4$@TiO$_2$/Pt nanocomposites as a candidate for photocatalytic applications.

CONFLICT OF INTEREST

The authors declare that there are no conflicts of interest regarding the publication of this manuscript.

REFERENCES

1. Saffarzadeh S, Nabiyouni G, Ghanbari D. Preparation of Ni(OH)2, NiO and NiFe2O4 nanoparticles: magnetic and photo-catalyst NiFe2O4-NiO nanocomposites. Journal of Materials Science: Materials in Electronics. 2016;27(12):13338-50.

2. Ahmadian Fard Fini S, Salavati-Niasari M, Safardoust-Hojaghan H. Precipitation green synthesis and photocatalytic activity of magnetic CoFe$_2$O$_4$–carbon quantum dots nanocomposite by turmeric precursor, J Mater Sci Mater Electron. 2017;28(21):16205–16214

3. Safardoust-Hojaghan H, Shakouri-Arani M, Salavati-Niasari M. Structural and spectroscopic characterization of HgS nanoparticles prepared via simple microwave approach in presence of novel sulfuring agent. Transactions of Nonferrous Metals Society of China. 2016;26(3):759-66.

4. Masoumi S, Nabiyouni G, Ghanbari D. Photo-degradation of azo dyes: photo catalyst and magnetic investigation of CuFe2O4-TiO2 nanoparticles and nanocomposites. Journal of Materials Science: Materials in Electronics. 2016;27(9):9962-75.

5. Masoumi S, Nabiyouni G, Ghanbari D. Photo-degradation of Congored, acid brown and acid violet: photo catalyst and magnetic investigation of CuFe2O4-TiO2-Ag nanocomposites. Journal of Materials Science: Materials in Electronics. 2016;27(10):11017-33.

6. Aliyan H, Fazaeli R, Jalilian R. Fe3O4@mesoporous SBA-15: A magnetically recoverable catalyst for photodegradation of malachite green. Applied Surface Science. 2013;276:147-53.

7. Buthiyappan A, Abdul Aziz AR, Wan Daud WMA. Recent advances and prospects of catalytic advanced oxidation process in treating textile effluents. Reviews in Chemical Engineering. 2016;32(1):1-47.

8. Liu S, Sun H, Ang HM, Tade MO, Wang S. Integrated oxygen-doping and dye sensitization of graphitic carbon nitride for enhanced visible light photodegradation. Journal of Colloid and Interface Science. 2016;476:193-9.

9. Bakre PV, Volvoikar PS, Vernekar AA, Tilve SG. Influence of acid chain length on the properties of TiO2 prepared by sol-gel method and LC-MS studies of methylene blue photodegradation. Journal of Colloid and Interface Science. 2016;474:58-67.

10. Wu X, Cai J, Li S, Zheng F, Lai Z, Zhu L, et al. Au@Cu 2 O stellated polytope with core-shelled nanostructure for high-performance adsorption and visible-light-driven photodegradation of cationic and anionic dyes. Journal of Colloid and Interface Science. 2016;469:138-46.

11. Alhaji MH, Sanaullah K, Lim S-F, Khan A, Hipolito CN, Abdullah MO, et al. Photocatalytic treatment technology for palm oil mill effluent (POME) - A review. Process Safety and Environmental Protection. 2016;102:673-86.

12. Ghanbari D, Salavati-Niasari M, Ghasemi-Kooch M. In situ and ex situ synthesis of poly(vinyl alcohol)-Fe 3 O 4 nanocomposite flame retardants. Particuology. 2016;26:87-94.

13. Goldman A. Modern Ferrite Technology, (Springer,New York, 2006).

14. Kinemuchi Y, Ishizaka K, Suematsu H, Jiang W, Yatsui K. Magnetic properties of nanosize NiFe2O4 particles synthesized by pulsed wire discharge. Thin Solid Films. 2002;407(1-2):109-13.

15. Nabiyouni G; Ghanbari D, Fe-Ag nanocomposite: Precipitation preparation of iron nanoparticles and silver dendrite like nanostructures . J Nanostruct. 2017; 7 (2): 11-120.

16. Khaghani S, Ghanbari D. Magnetic and photo-catalyst Fe3O4-Ag nanocomposite: green preparation of silver and magnetite nanoparticles by garlic extract. Journal of Materials Science: Materials in Electronics. 2016;28(3):2877-86.

17. Nabiyouni G; Ghanbari D; Ghasemi J; Yousofnejad A, Microwave-assisted Synthesis of MgFe$_2$O$_4$-ZnO Nanocomposite and Its Photo-catalyst Investigation in Methyl Orange Degradation. J Nanostruct. 2015; 5 (3): 289-295.

18. Ghanbari D, Salavati-Niasari M. Synthesis of urchin-like CdS-Fe3O4 nanocomposite and its application in flame retardancy of magnetic cellulose acetate. Journal of Industrial and Engineering Chemistry. 2015;24:284-92.

19. Hassanpour M, Safardoust-Hojaghan H, Salavati-Niasari M, Yeganeh-Faal A. Nano-sized CuO/ZnO hollow spheres: synthesis, characterization and photocatalytic performance. Journal of Materials Science: Materials in Electronics. 2017;28(19):14678-84.

20. Hassanpour M, Safardoust H, Ghanbari D, Salavati-Niasari M. Microwave synthesis of CuO/NiO magnetic nanocomposites and its application in photo-degradation of methyl orange. Journal of Materials Science: Materials in Electronics. 2015;27(3):2718-27.